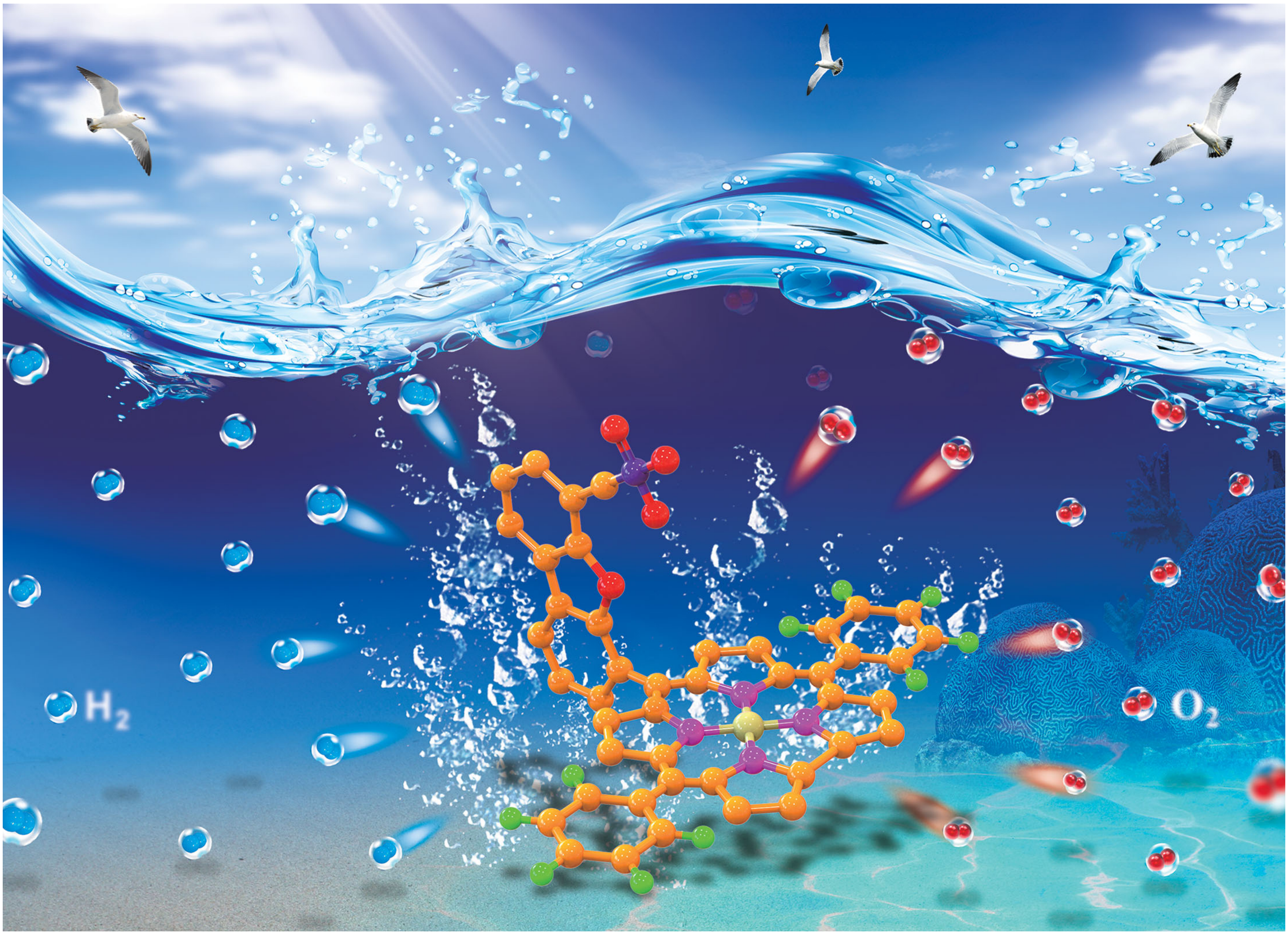

Showcasing research from the laboratory of Professor Rui Cao at the Department of Chemistry, Renmin University of China, Beijing and at the School of Chemistry and Chemical Engineering, Shaanxi Normal University, Xi'an, China.

Cobalt corroles with phosphonic acid pendants as catalysts for oxygen and hydrogen evolution from neutral aqueous solution

Cobalt corroles with phosphonic acid pendants showed improved activities in both oxygen and hydrogen evolution from neutral aqueous solutions, highlighting the importance of the secondary coordination sphere in catalyst design.

As featured in:


Volume 53 | Number 46 | 11 June 2017 | Pages 6177–6278

ChemComm

Chemical Communications
rsc.li/chemcomm

ISSN 1359-7345

ROYAL SOCIETY OF CHEMISTRY

COMMUNICATION
Luis M. Campos, Wei Min et al.
Stimulated Raman scattering of polymer nanoparticles for multiplexed live-cell imaging

See Rui Cao *et al*.,
Chem. Commun., 2017, **53**, 6195.

ROYAL SOCIETY OF CHEMISTRY

rsc.li/chemcomm

ChemComm

COMMUNICATION

View Article Online
View Journal | View Issue

Cite this: *Chem. Commun.*, 2017, **53**, 6195

Received 29th March 2017,
Accepted 26th April 2017

DOI: 10.1039/c7cc02400b

rsc.li/chemcomm

Cobalt corroles with phosphonic acid pendants as catalysts for oxygen and hydrogen evolution from neutral aqueous solution†

Huiling Sun,‡[a] Yongzhen Han,‡[a] Haitao Lei,[a] Mingxing Chen[a] and Rui Cao *[ab]

Cobalt corroles with different acid/base pendants, L^{Br}–Co, L^{COOH}–Co, $L^{PO(OH)_2}$–Co, and $L^{CH_2PO(OH)_2}$–Co (L = 5,15-bis-(pentafluorophenyl)-10-(4-dibenzofuran)corrole), were synthesized and examined as catalysts for oxygen and hydrogen evolution from neutral aqueous solutions. Co corroles with phosphonic acid pendants showed improved activities in both processes, highlighting the importance of the secondary coordination sphere in catalyst design.

An attractive way to meet the growing global energy demand is to convert solar energy to chemical fuels.[1,2] Water splitting is an ideal protocol for this solar-to-fuel strategy.[3,4] However, its two half reactions, the oxygen evolution reaction (OER) and hydrogen evolution reaction (HER), are kinetically slow.[3,4] Therefore, designing cheap and efficient OER[4,5] and HER[6,7] catalysts has attracted extensive attention. A variety of molecular catalysts of Mn,[8–10] Fe,[11–13] Co,[14–26] Ni,[27–31] and Cu[32–35] have been identified as OER and/or HER catalysts. Particular emphases have been placed on providing new insights into catalyst design to reveal the structure–function relationship.

Metallocorroles have been shown to be highly active for OER[3,9,14,15,17] and HER.[3,22,23,32] Trianionic corrole ligands can afford a stable square-planar coordination mode and are very effective in stabilizing high-valent metal ions, which are usually involved in OER.[3] Consequently, corrole ligands can offer low-valent metal ions large reducing powers. All these features make metal corroles attractive for OER and HER catalysis.

In addition, the second coordination sphere of metal ions has a substantial effect on catalysis.[36] For example, DuBois and co-workers demonstrated that pendant amines proximate to the metal ion can significantly improve the catalytic efficiency of Ni-based HER catalysts.[29,30] Protonated amine groups can function as intramolecular proton relays to facilitate proton transfer processes. Nocera and co-workers designed hangman metalloporphyrins as HER catalysts and showed that the hanging carboxyl acid group is able to assist HER by mediating proton-coupled electron transfer (PCET) steps.[11,21] These authors further revealed that the rate of HER catalysis is affected by the proton-donating ability of the hanging group. For OER, Nocera and co-workers showed that the hanging carboxyl group can increase the catalytic activity of Co corroles.[17] Theoretical studies by Cramer[37] and us[38] suggested that the carboxyl group in the second coordination sphere of the Co ion can act as an intramolecular base to assist the rate-limiting O–O bond formation through a concerted oxygen atom-proton transfer mechanism.[33,39] However, due to synthetic challenges to introduce functional groups into the second coordination sphere of metal ions, few examples have been reported to compare the effects of different acid/base pendants on OER and HER catalysis.

It is known that the increase of the proton-accepting ability of the base will increase the O–O bond formation rate.[3] We are thus interested in attaching phosphonic acid groups to the second coordination sphere of Co corroles. As the pK_{a2} of phosphonic acid groups is larger than the pK_a of carboxyl acid groups, Co corroles with phosphonic acid pendants are considered to have improved OER activities as compared to analogues without such groups. In addition, because of the different proton-donating abilities of phosphonic and carboxyl acid groups, it is intriguing to study the HER activity of Co corroles with phosphonic acid pendants. Herein we report the syntheses and characterization of four Co corroles appended with different acid/base groups. Complexes L^{Br}–Co, L^{COOH}–Co, $L^{PO(OH)_2}$–Co, and $L^{CH_2PO(OH)_2}$–Co all have an active Co corrole site attached to the 4-position of the dibenzofuran unit and have different pendants at its 6-position (Scheme 1). All these complexes are active for OER and HER from neutral aqueous solutions. Our results show that appended groups at the 6-position of dibenzofuran play crucial roles in both processes. Complex $L^{CH_2PO(OH)_2}$–Co outperforms others in

---

[a] *Department of Chemistry, Renmin University of China, Beijing 100872, China. E-mail: ruicao@ruc.edu.cn*

[b] *School of Chemistry and Chemical Engineering, Shaanxi Normal University, Xian 710119, China*

† Electronic supplementary information (ESI) available: Details for the syntheses and characterization of all complexes, X-ray data as CIF files, Schemes S1–S4, Tables S1–S3 and Fig. S1–S76. CCDC 1526192–1526195. For ESI and crystallographic data in CIF or other electronic format see DOI: 10.1039/c7cc02400b

‡ These authors contributed equally to this work.

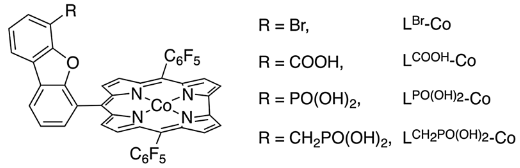

Scheme 1 Molecular structures of Co corroles. Pyridine groups bound to the axial positions of Co are omitted for clarity.

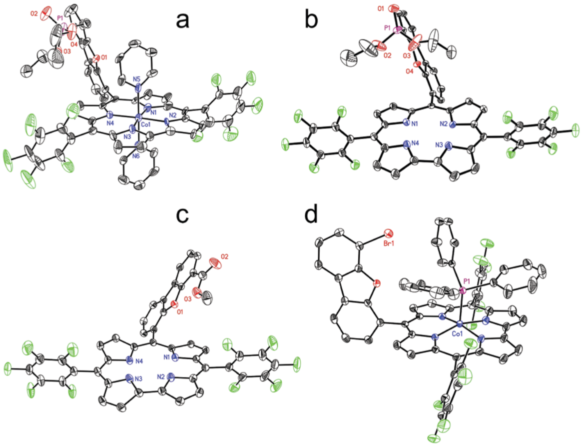

Fig. 1 Thermal ellipsoid plot (50% probability) of the X-ray structures of (a) $\mathrm{L}^{\mathrm{CH_2PO(OEt)_2}}$–Co, (b) $\mathrm{L}^{\mathrm{PO(OEt)_2}}$, (c) $\mathrm{L}^{\mathrm{COOMe}}$, and (d) L^{Br}–Co–$\mathrm{PPh_3}$.

both OER and HER. This work therefore highlights the importance of the secondary coordination sphere in catalyst design.

The synthetic routes of the four Co corroles are depicted in Scheme 2. For $\mathrm{L}^{\mathrm{CH_2PO(OH)_2}}$–Co, the introduction of two formyl groups at 4- and 6-positions of dibenzofuran was realized by treating it with *n*-BuLi followed by reaction with dimethylformamide (DMF, route A). Details of synthesis and characterization are given in the ESI.† One of the formyl groups was converted to –$\mathrm{CH_2PO(OEt)_2}$, and the other one was converted to a corrole unit containing two pentafluorophenyl units at its 5- and 15-positions. The subsequent hydrolysis and reaction with $\mathrm{Co(OAc)_2}$ gave $\mathrm{L}^{\mathrm{CH_2PO(OH)_2}}$–Co. Its identity and purity were confirmed by NMR spectroscopy (Fig. S46 and S47, ESI†) and high-resolution mass spectrometry (HRMS, Fig. S48, ESI†). Attempts to grow crystals of $\mathrm{L}^{\mathrm{CH_2PO(OH)_2}}$–Co for X-ray analysis were not successful. Instead, we synthesized its ester form $\mathrm{L}^{\mathrm{CH_2PO(OEt)_2}}$–Co for structural studies (^{1}H NMR, Fig. S49; HRMS, Fig. S50, ESI†).

Complex $\mathrm{L}^{\mathrm{CH_2PO(OEt)_2}}$–Co crystallized in the orthorhombic space group $P2_12_12$ (cell parameters in Table S1, ESI†). The Co ion is coordinated by the four N atoms of the corrole unit, which define an equatorial plane (Fig. 1a). Two additional pyridine groups are bound to the axial positions of Co. The resulting octahedral coordination environment and short Co–N bond distances are indicative of a d^6 Co$^{\mathrm{III}}$ electronic configuration,[15] which is consistent with the diamagnetism of $\mathrm{L}^{\mathrm{CH_2PO(OEt)_2}}$–Co as established by ^{1}H NMR. Because $\mathrm{L}^{\mathrm{CH_2PO(OEt)_2}}$–Co and $\mathrm{L}^{\mathrm{CH_2PO(OH)_2}}$–Co should have very similar structural aspects except that the –$\mathrm{CH_2PO(OEt)_2}$ moiety is converted to –$\mathrm{CH_2PO(OH)_2}$ in the latter complex, the place and orientation and also the distance of the –$\mathrm{CH_2PO(OH)_2}$ unit to Co can be estimated based on the X-ray structure of $\mathrm{L}^{\mathrm{CH_2PO(OEt)_2}}$–Co. Structural analysis showed that the distance of the phosphonic oxygen atoms to Co is about 6.6 Å, indicating that they are close enough to Co to potentially act as an

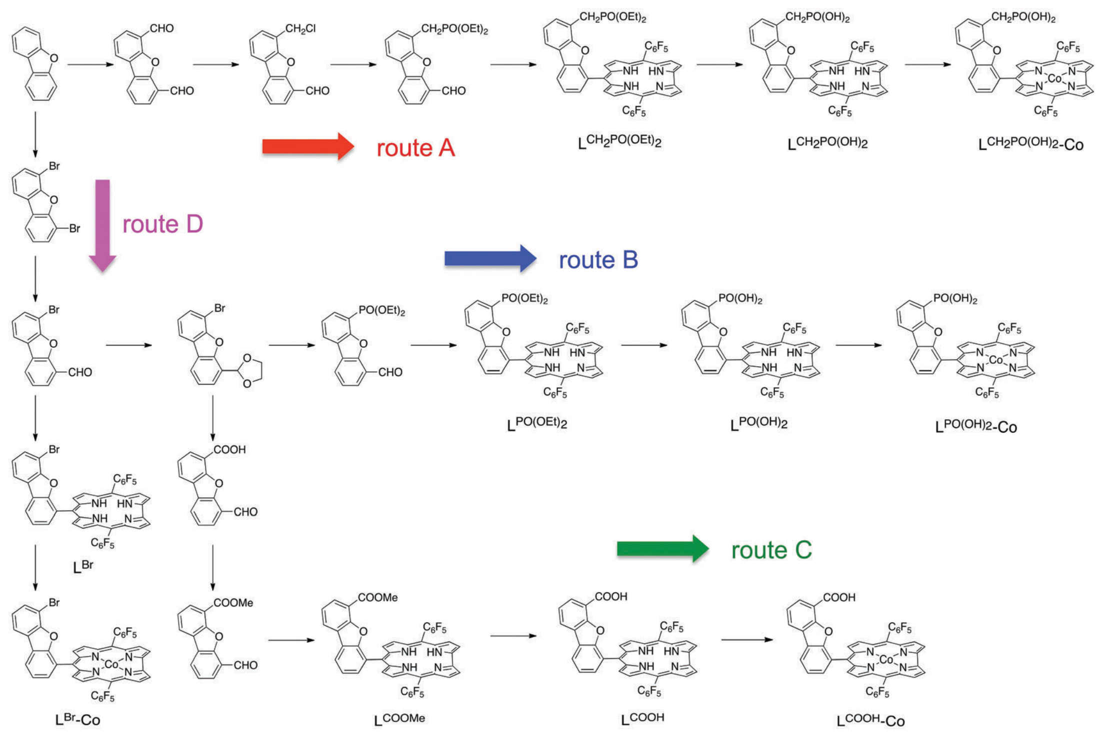

Scheme 2 Synthetic routes of $\mathrm{L}^{\mathrm{CH_2PO(OH)_2}}$–Co (route A), $\mathrm{L}^{\mathrm{PO(OH)_2}}$–Co (route B), $\mathrm{L}^{\mathrm{COOH}}$–Co (route C), and L^{Br}–Co (route D).

intramolecular base to facilitate the nucleophilic attack of a water molecule to a Co-oxo unit for O–O bond formation.[33,39]

Co corrole $L^{PO(OH)_2}$–Co was synthesized following route B (Scheme 2). Complex 4,6-dibromodibenzofuran was treated with one equiv. of PhLi followed by reaction with DMF to give 4-formyl-6-bromodibenzofuran. The subsequent conversion of –Br to $-PO(OEt)_2$ and conversion of –CHO to corrole were realized. The resulting $L^{PO(OEt)_2}$ was structurally characterized (cell parameters in Table S1, ESI†), showing an appended $-PO(OEt)_2$ group proximate to a corrole unit (Fig. 1b). The corresponding $L^{PO(OH)_2}$–Co was characterized by NMR (Fig. S31 and S32, ESI†) and HRMS (Fig. S33, ESI†). Starting from 4-formyl-6-bromodibenzofuran, –Br could be converted to –COOMe (route C). L^{COOMe} was structurally characterized (Fig. 1c, cell parameters in Table S1, ESI†). The corresponding L^{COOH}–Co was also carefully characterized (Fig. S19 and S20, ESI†). Additionally, L^{Br}–Co was synthesized as an analogue lacking acid/base pendants (route D, ^{1}H NMR, Fig. S7; HRMS, Fig. S8, ESI†). In order to grow crystals of L^{Br}–Co, one equiv. of PPh_3 was added. The resulting L^{Br}–Co–PPh_3 crystallized in the orthorhombic space group *Pbca* (Fig. 1d, cell parameters in Table S1, ESI†). The Co ion has a square pyramidal coordination environment with the four N atoms of corrole defining the equatorial plane and PPh_3 occupying the axial position.

On the basis of structural studies of $L^{CH_2PO(OEt)_2}$–Co, $L^{PO(OEt)_2}$, L^{COOMe}, and L^{Br}–Co–PPh_3, we can conclude that four complexes contain different acid/base pendants proximate to corrole units. The dibenzofuran unit is therefore valuable to make functional groups at the second coordination sphere of metal centers. It is worth noting that the two *meso*-C_6F_5 substituents have strong electron-withdrawing features. The use of *meso*-C_6F_5 substituents is aimed to (1) decrease the electron density of the corrole ring and thus increase its stability during OER and (2) shift the redox events of corroles to the anodic direction to reduce the overpotential for HER.

Cyclic voltammograms (CVs) of Co corroles were recorded in acetonitrile (0.1 M Bu_4NPF_6). Due to the very low solubility of $L^{PO(OH)_2}$–Co and $L^{CH_2PO(OH)_2}$–Co, their ester forms were used for CV measurements. In general, these Co corroles each showed four redox events (Fig. S55–S58, data summarized in Table S3, ESI†). As can be seen from these data, the redox potentials of these Co corroles are almost identical. These results demonstrate that pendants at the second coordination sphere of Co ions have small influence on the redox potentials. It is worth noting that the second reduction wave of L^{COOH}–Co is irreversible. This result indicates the reduction of the acid protons. A similar observation was reported by Nocera and co-workers on hangman metalloporphyrins.[21]

Catalytic OER was performed in 0.1 M pH 7 phosphate buffers using catalyst-coated fluorine-doped tin oxide (FTO) working electrodes. The amount of catalysts loaded on FTO is intended to be 20 nmol cm^{-2}. Fig. 2a shows that the OER activity has the order of $L^{CH_2PO(OH)_2}$–Co > $L^{PO(OH)_2}$–Co > L^{COOH}–Co > L^{Br}–Co. The onset potential of the catalytic wave with $L^{CH_2PO(OH)_2}$–Co is 1.27 V *vs.* normal hydrogen electrode (NHE, all potentials reported are *vs.* NHE unless otherwise noted), corresponding to an onset overpotential of 450 mV. This value is smaller than those of other Co corrole OER catalysts reported in the literature.[15,17] The appended base group is considered to be able to act as an intramolecular base to assist the O–O bond formation through a concerted oxygen atom-proton transfer mechanism. Because $ArCH_2PO_3^{2-}$ (pK_{a2} of $ArCH_2PO_3H_2$ *ca.* 8.4) is more basic than others in this series (pK_{a2} of $ArPO_3H_2$ *ca.* 7.1, pK_a of ArCOOH *ca.* 4.2), it is more effective in facilitating the O–O bond formation. Fig. 2b shows the plot of potential (measured at 0.52 mA cm^{-2}) *vs.* pK_a of appended groups (for $-PO(OH)_2$ and $-CH_2PO(OH)_2$, pK_{a2} are used). The slope is the −55 mV per pK_a unit. A similar observation was reported by Groves and Wang: plotting the potential at a fixed current *vs.* pK_a of the buffer anion gave a slope of −54 mV per pK_a.[16] These results indicate that the OER mechanism involves a rate-determining PCET step (*i.e.*, O–O bond formation), in which the electron transfer process becomes more favorable because of the improved proton transfer process as facilitated by a stronger basic group.[16,17,39] Controlled potential electrolysis (CPE) studies were then carried out to examine the stability of these Co corroles during OER (Fig. S59–S62, ESI†). During 5 h CPE, currents remained relatively stable. The Faradaic efficiencies of all four Co corroles for O_2 evolution were measured to be more than 90% (Fig. S69–S72, ESI†). In addition, the washed FTO electrodes after electrolysis exhibited no catalytic OER activities, and no heterogeneous particles were formed on the washed electrodes as examined by scanning electron microscopy (SEM) and energy dispersive X-ray spectroscopy (EDX) (Fig. S67, ESI†). All these results suggest the molecular nature of these Co corroles for OER catalysis.

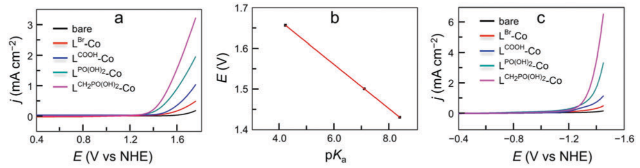

Fig. 2 (a) Linear sweep voltammetry (LSV) of OER using blank and catalyst-coated (20 nmol cm^{-2}) FTO electrodes in 0.1 M pH 7 phosphate buffers. (b) The plot of potential at 0.52 mA cm^{-2} *vs.* pK_a of appended groups. (c) LSV of HER using blank and catalyst-coated (70 nmol cm^{-2}) GC electrodes in 0.1 M pH 7 phosphate buffers.

Catalytic HER with these Co corroles was also examined using catalyst-coated glassy carbon (GC) electrodes in 0.1 M pH 7 phosphate buffers. The amount of catalysts loaded on GC is intended to be 70 nmol cm^{-2}. Our results give an activity order of $L^{CH_2PO(OH)_2}$–Co > $^{PO(OH)_2}$–Co > L^{COOH}–Co > ^{Br}–Co (Fig. 2c). This trend is likely due to the higher protonation level of $-CH_2PO_3^{2-}$ in neutral aqueous solutions, which leads to an effectively higher local proton concentration.[11] Similarly, their stabilities for HER were examined by CPE studies, which gave almost stable current profiles (Fig. S63–S66, ESI†). The Faradaic efficiencies for H_2 evolution were determined to be larger than 80% (*i.e.*, for $L^{CH_2PO(OH)_2}$–Co, it is 94%, Fig. S73–S76, ESI†). The washed GC electrodes after electrolysis were not active for HER and showed no heterogeneous phases in SEM and EDX analyses (Fig. S68, ESI†). All these results suggest that these Co corroles are real catalysts for HER. It is necessary to note that Co corroles have been verified to be robust for both OER and HER in previous reports by others[17,22] and us.[14,15]

In summary, four Co corroles with different acid/base pendants were synthesized and characterized. Catalytic OER and HER studies from neutral aqueous solutions showed that $L^{CH_2PO(OH)_2}$–Co is the most active one in this series of complexes. The $-CH_2PO(OH)_2$ group can act as an intramolecular base to assist the O–O bond formation in OER and can act as a proton pond to increase the effective local proton concentration in HER. Our results therefore highlight the importance of the secondary coordination sphere in catalyst design.

We are grateful for the support from the ''Thousand Talents Program'' of China, the National Natural Science Foundation of China under Grants 21101170 and 21573139, the Fundamental Research Funds for the Central Universities, and the Research Funds of Renmin University of China.

Notes and references

1 D. Gust, T. A. Moore and A. L. Moore, *Acc. Chem. Res.*, 2009, **42**, 1890–1898.
2 T. R. Cook, D. K. Dogutan, S. Y. Reece, Y. Surendranath, T. S. Teets and D. G. Nocera, *Chem. Rev.*, 2010, **110**, 6474–6502.
3 W. Zhang, W. Z. Lai and R. Cao, *Chem. Rev.*, 2017, **117**, 3717–3797.
4 M. D. Kärkäs, O. Verho, E. V. Johnston and B. Åkermark, *Chem. Rev.*, 2014, **114**, 11863–12001.
5 R. Cao, W. Z. Lai and P. W. Du, *Energy Environ. Sci.*, 2012, **5**, 8134–8157.
6 J. R. McKone, S. C. Marinescu, B. S. Brunschwig, J. R. Winkler and H. B. Gray, *Chem. Sci.*, 2014, **5**, 865–878.
7 V. S. Thoi, Y. J. Sun, J. R. Long and C. J. Chang, *Chem. Soc. Rev.*, 2013, **42**, 2388–2400.
8 Y. Shimazaki, T. Nagano, H. Takesue, B. H. Ye, F. Tani and Y. Naruta, *Angew. Chem., Int. Ed.*, 2004, **43**, 98–100.
9 W. Schöfberger, F. Faschinger, S. Chattopadhyay, S. Bhakta, B. Mondal, J. A. A. W. Elemans, S. Müllegger, S. Tebi, R. Koch, F. Klappenberger, M. Paszkiewicz, J. V. Barth, E. Rauls, H. Aldahhak, W. G. Schmidt and A. Dey, *Angew. Chem., Int. Ed.*, 2016, **55**, 2350–2355.
10 E. A. Karlsson, B. L. Lee, T. Åkermark, E. V. Johnston, M. D. Kärkäs, J. L. Sun, Ö. Hansson, J. E. Bäckvall and B. Åkermark, *Angew. Chem., Int. Ed.*, 2011, **50**, 11715–11718.
11 D. J. Graham and D. G. Nocera, *Organometallics*, 2014, **33**, 4994–5001.
12 J. L. Fillol, Z. Codolà, I. Garcia-Bosch, L. Gómez, J. J. Pla and M. Costas, *Nat. Chem.*, 2011, **3**, 807–813.
13 M. J. Rose, H. B. Gray and J. R. Winkler, *J. Am. Chem. Soc.*, 2012, **134**, 8310–8313.
14 H. T. Lei, C. Y. Liu, Z. J. Wang, Z. Y. Zhang, M. N. Zhang, X. M. Chang, W. Zhang and R. Cao, *ACS Catal.*, 2016, **6**, 6429–6437.
15 H. T. Lei, A. L. Han, F. W. Li, M. N. Zhang, Y. Z. Han, P. W. Du, W. Z. Lai and R. Cao, *Phys. Chem. Chem. Phys.*, 2014, **16**, 1883–1893.
16 D. Wang and J. T. Groves, *Proc. Natl. Acad. Sci. U. S. A.*, 2013, **110**, 15579–15584.
17 D. K. Dogutan, R. McGuire Jr. and D. G. Nocera, *J. Am. Chem. Soc.*, 2011, **133**, 9178–9180.
18 J. P. Bigi, T. E. Hanna, W. H. Harman, A. Chang and C. J. Chang, *Chem. Commun.*, 2010, **46**, 958–960.
19 B. B. Beyene, S. B. Mane and C. H. Hung, *Chem. Commun.*, 2015, **51**, 15067–15070.
20 J. G. Kleingardner, B. Kandemir and K. L. Bren, *J. Am. Chem. Soc.*, 2014, **136**, 4–7.
21 C. H. Lee, D. K. Dogutan and D. G. Nocera, *J. Am. Chem. Soc.*, 2011, **133**, 8775–8777.
22 B. Mondal, K. Sengupta, A. Rana, A. Mahammed, M. Botoshansky, S. G. Dey, Z. Gross and A. Dey, *Inorg. Chem.*, 2013, **52**, 3381–3387.
23 A. Mahammed, B. Mondal, A. Rana, A. Dey and Z. Gross, *Chem. Commun.*, 2014, **50**, 2725–2727.
24 T. Nakazono, A. R. Parent and K. Sakai, *Chem. Commun.*, 2013, **49**, 6325–6327.
25 P. L. Zhang, M. Wang, F. Gloaguen, L. Chen, F. Quentel and L. C. Sun, *Chem. Commun.*, 2013, **49**, 9455–9457.
26 L. Chen, M. Wang, K. Han, P. L. Zhang, F. Gloaguen and L. C. Sun, *Energy Environ. Sci.*, 2014, **7**, 329–334.
27 Y. Z. Han, H. Y. Fang, H. Z. Jing, H. L. Sun, H. T. Lei, W. Z. Lai and R. Cao, *Angew. Chem., Int. Ed.*, 2016, **55**, 5457–5462.
28 Y. Z. Han, Y. Z. Wu, W. Z. Lai and R. Cao, *Inorg. Chem.*, 2015, **54**, 5604–5613.
29 M. L. Helm, M. P. Stewart, R. M. Bullock, M. R. DuBois and D. L. DuBois, *Science*, 2011, **333**, 863–866.
30 U. J. Kilgore, J. A. S. Roberts, D. H. Pool, A. M. Appel, M. P. Stewart, M. R. DuBois, W. G. Dougherty, W. S. Kassel, R. M. Bullock and D. L. DuBois, *J. Am. Chem. Soc.*, 2011, **133**, 5861–5872.
31 P. L. Zhang, M. Wang, Y. Yang, D. H. Zheng, K. Han and L. C. Sun, *Chem. Commun.*, 2014, **50**, 14153–14156.
32 H. T. Lei, H. Y. Fang, Y. Z. Han, W. Z. Lai, X. F. Fu and R. Cao, *ACS Catal.*, 2015, **5**, 5145–5153.
33 M. K. Coggins, M.-T. Zhang, Z. F. Chen, N. Song and T. J. Meyer, *Angew. Chem., Int. Ed.*, 2014, **53**, 12226–12230.
34 S. M. Barnett, K. I. Goldberg and J. M. Mayer, *Nat. Chem.*, 2012, **4**, 498–502.
35 P. L. Zhang, M. Wang, Y. Yang, T. Y. Yao and L. C. Sun, *Angew. Chem., Int. Ed.*, 2014, **53**, 13803–13807.
36 M. R. DuBois and D. L. DuBois, *Chem. Soc. Rev.*, 2009, **38**, 62–72.
37 M. Z. Ertem and C. J. Cramer, *Dalton Trans.*, 2012, **41**, 12213–12219.
38 W. Z. Lai, R. Cao, G. Dong, S. Shaik, J. N. Yao and H. Chen, *J. Phys. Chem. Lett.*, 2012, **3**, 2315–2319.
39 Z. F. Chen, J. J. Concepcion, X. Q. Hu, W. T. Yang, P. G. Hoertz and T. J. Meyer, *Proc. Natl. Acad. Sci. U. S. A.*, 2010, **107**, 7225–7229.